*Nanotechnology Perceptions*
*ISSN 1660-6795*
*www.nano-ntp.com*

# Expired Medicine-derived Green Synthesis of Zinc Oxide (ZnO) Nanoparticles for its applications from Semiconductor to Biomedical Applications

**Naveen Kumar[1], **Rakesh Kumar Singh[1], Vivek Kumar[2], Shachi Mishra[3]**

*[1]Aryabhatta Center for Nanoscience and Nanotechnology, Aryabhatta Knowledge University, India*
*[2]Department of Electronics and Communication Engineering, Vidya Vihar Institute of Technology, Maranga, Purnea, India*
*[3]Department of Chemistry, Jai Prakash University Chapra, India*
**** Corresponding Author**: Dr. Rakesh Kumar Singh*

***Abstract:***

Green synthesis, an alternative to traditional chemical methods, is gaining importance due to its cost-effectiveness, reduced environmental impact, and broad medicinal capabilities. The present research describes the synthesis of Zinc oxide nanoparticles (ZnO NPs) from waste-derived expired drugs (Norflox TZ, Metrogyl, Betnosol and Combiflam). The crystallite size was found to range from 39 nm to 44 nm. ZnO synthesized using expire medicine Norflox TZ displayed the highest crystallinity with a hexagonal crystal structure belonging to the P 63 m c space group. The Tauc plot was used to compute the band gap of the ZnO NPs created from expired pharmaceuticals, yielding a range from 1.47 eV to 1.5 eV. The FTIR spectra indicated wavenumbers ranging from 471 cm-1 to 3500 cm-1. The SEM images reflected the agglomeration in the prepared ZnO nanomaterials. The research findings revealed that ZnO nanoparticles (NPs) synthesized from expired medications demonstrated significant antimicrobial activity. Among the antibacterial results, Pseudomonas aeruginosa exhibited the highest inhibition zone (24.2 ± 1.16 mm) with ZnO NPs synthesized using Norflox TZ. In the antifungal analysis, Penicillium citrinum showed the largest inhibition zone (28.2 ± 0.68 mm) with Norflox TZ-derived ZnO NPs. These results underscore the potential of ZnO NPs for effective antimicrobial applications, particularly using Norflox TZ synthesis for enhanced efficacy. Thus, the prepared ZnO nanomaterials prepared from expired medicines may be useful from semiconductor industries to Biomedical applications.

**Keywords:** Green synthesis, Expired medicines, ZnO NPs, Semiconductor Band gap, Antibacterial, Antifungal

## 1. Introduction

Nanotechnology refers to the art and science of manipulating materials at the nano-scale

regime to create unique materials with immense potential of transforming society [1-2]. Nanoparticles (NPs) have found extensive applications in various fields like optics, cosmetics, electronics, magnets, biomolecule detection, sunscreen lotions, diagnostics, and medicine [3-5]. Inorganic NPs like Ag, Cu, Au, $TiO_2$, and ZnO are versatile and can be utilized for activities such as anti-diabetic, anti-cancer, and antibacterial effects [6-9]. ZnO NPs possess various biomedical properties such as antimicrobial activity and are used in beauty products, dental pain relief, diagnostics, and microbial pollution prevention with semiconductor properties [10-12]. ZnO NPs exhibit remarkable antimicrobial effects against viruses, fungi, and bacteria, making them suitable for food industry applications as surface coatings. Numerous methods, including standard ceramic, hydrothermal, bio-synthesis, co-precipitation, sol-gel, and micro-emulsion, are employed by researchers to synthesize NPs [13]. However, NPs produced through physical and chemical methods often involve toxic chemicals and are costly [14]. As a greener approach, Ramesh et al. prepared ZnO nanoparticles from the leaf extract of Cassia auriculata leaf [15]. Besides this, there are several reports of synthesis of ZnO materials using different synthesis methods for controlling size, morphology and band gap engineering [17-21].

Expired medicines, which are commonly discarded, often retain much of their potential effectiveness. The expiration date guarantees the drug will remain potent until that specified date. However, research shows that when stored properly, drug maintain 90% of their potency for at least five years after the labelled expiry date, and sometimes even longer [16]. Many drugs retain their original potency even a decade after the expiration date. The term "expiry" refers to a medication's shelf life or therapeutic effectiveness, and the disposal of expired medicines can lead to environmental pollution. When discarded in the open, they contribute to air pollution, and when disposed into water bodies, they not only contaminate the water but can also lead to drug-resistant waterborne bacteria. Therefore, in the present research, we envisioned to employ waste expired medicines to prepare the ZnO nanomaterials with the objective to reduce the pollution caused by the expired medicines and evaluate their properties for semiconductor and biomedical applications, thus aiming for waste to wealth generation.

While nanoscience and technology are progressively seeking environmentally friendly synthesis methods for novel nanomaterials, previous attempts have been made to synthesize metals, metal oxides, and chalcogenides nanoparticles using expired medicines [17]. It is believed that although a drug may lose its therapeutic effectiveness, its chemical properties remain intact, and under suitable physicochemical conditions, it can produce nanomaterials. As a result, we have chosen to employ a green synthesis method to create ZnO NPs from commonly used expired medicines such as norflox TZ, metrogyl, betnosol, and combiflam, which are otherwise treated as waste. This innovative approach is of paramount significance as it tackles the hazardous effects associated with the disposal of such medicines which include air contamination upon outdoor disposal and the potential alteration of waterborne microbes, rendering them resistant to certain medications. Furthermore, nanomaterials synthesized using this approach exhibit enhanced efficacy due to functionalization by the residual pharmaceutical ingredients, leading to significantly higher functional potential.

## 2. Materials and Method

2.1 Collection of expired medicines

After analyzing the manufacture and expiry dates, 4–6-month-old medicine was collected from various pharmacy outlets in Patna, Bihar, India.

2.2 Preparation of the expired medicine extract

Based on molecular weight, 4–6-month expired Metrogyl, Norflox TZ, Betnosol, and Combiflam tablets were dissolved slowly in 200 mL sterile distilled water and 5 mL N/20 HCl was added to ensure a better degree of dissolution through gentle heating over a steam bath of up to 40°C until a light-yellow color appeared in the conical flask. The expired pharmaceutical extract was allowed to cool to ambient temperature before being kept for future research.

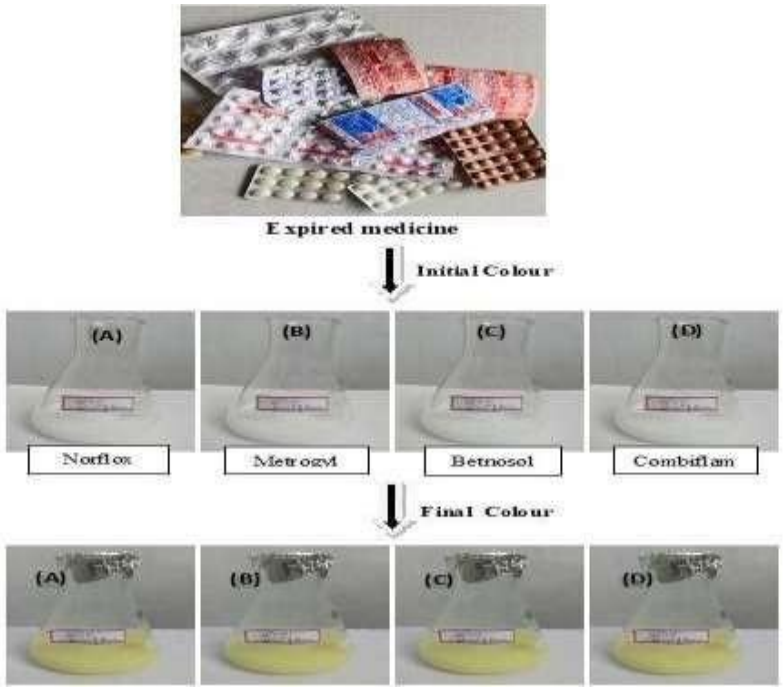


Fig1. Visual observation of ZnO nanoparticles synthesis using waste Expire medicine

2.3 Synthesis of Zinc nanoparticles

To begin the experiment, a beaker was filled with 100 ml of extract from expired medicine. The pH of the solution was carefully adjusted to a range of 4 to 6 using sodium bicarbonate ($NaHCO_3$). After that, the mixture was stirred for an hour at 70 °C. Following the conclusion of the stirring, a freshly produced solution of zinc chloride salt was added, and the continuous stirring was kept at the same temperature for another hour. After attaining the ideal thermodynamic conditions for further reactions, a tiny amount of sodium hydroxide (NaOH) pellets was added to bring the pH to 6. After two hours of stirring, the solution developed a distinct yellow colour, indicating the effective synthesis of ZnO nanoparticles (ZnO NPs). The precipitate that resulted was rigorously filtered before being dried in a hot air-dry oven at 60°C

for 2 hours. The dried nanoparticles were safely kept in an airtight container for future research and their properties were measured using modern scientific tools.

2.4 Characterization of green synthesized ZnO NPs

Optical properties of ZnO NPs were characterized based on UV absorption spectra (PerkinElmer Lamda 950) with the wavelength range of 300-500 nm, and X-ray diffraction (XRD) analysis was performed on an X-ray diffractometer (PAN analytical XRD) operating at 30 kV and 40 mA. All the sample was scanned from a 20 to 70-degree diffraction angle. 2 mg of ZnO NPs was mixed with 200 mg of potassium bromide (FTIR grade) and pressed into a pellet for FTIR characterization. The sample pellet was placed into the sample holder, and FTIR spectra were recorded in FTIR spectroscopy instrument (PerkinElmer Frontier) at a resolution of 4 $cm^{-1}$.

2.5 Antimicrobial activity of green synthesized ZnO NPs

The well diffusion method tested the antibacterial and antifungal activity of synthesized ZnO NPs against 4 bacteria such as Pseudomonas aeruginosa, Staphylococcus aureus, Escherichia coli and Bacillus cereus and 4 fungal strain Aspergillus niger, Candida albicans, Fusarium oxysporium and Penicillium citirinum. Bacterial strains were grown and maintained on nutrient agar medium, while fungi were maintained on potato dextrose agar (PDA) medium. Each strain's new overgrowth culture was swabbed uniformly onto the various plates. 30 ml of ZnO nanoparticles solution impregnated disc were placed on the plates and the varied levels of zonation generated around the well were measured.

## 3. Results and Discussion

3.1 UV-visible analysis

Figure 2 (a-d) shows the absorbance spectra of synthesized ZnO nanoparticles using expired medicines. The ultraviolet (UV) area exhibits strong absorption notably at 322 nm for Metrogyl, 269 nm for Norflox TZ, 247 nm for Betnesol, and 251 nm for Combiflam. This absorption peak in the UV range could be caused by the conversion of incident radiation into surface plasmons at the particle-medium interface. The width of the peak shows that ZnO NPs formed from expired drugs have a uniform distribution and a wide range of sizes [18]. The form, size, and dielectric properties of the surrounding media all influence the surface plasmon resonance (SPR) phenomena in ZnO NPs. A Tauc plot analysis, Fig. 3 (a-d) was used to determine the band gap. The Tauc plot is given by the following equation:

$$\alpha h\nu = B\,(h\nu - E_g)^n \quad (1)$$

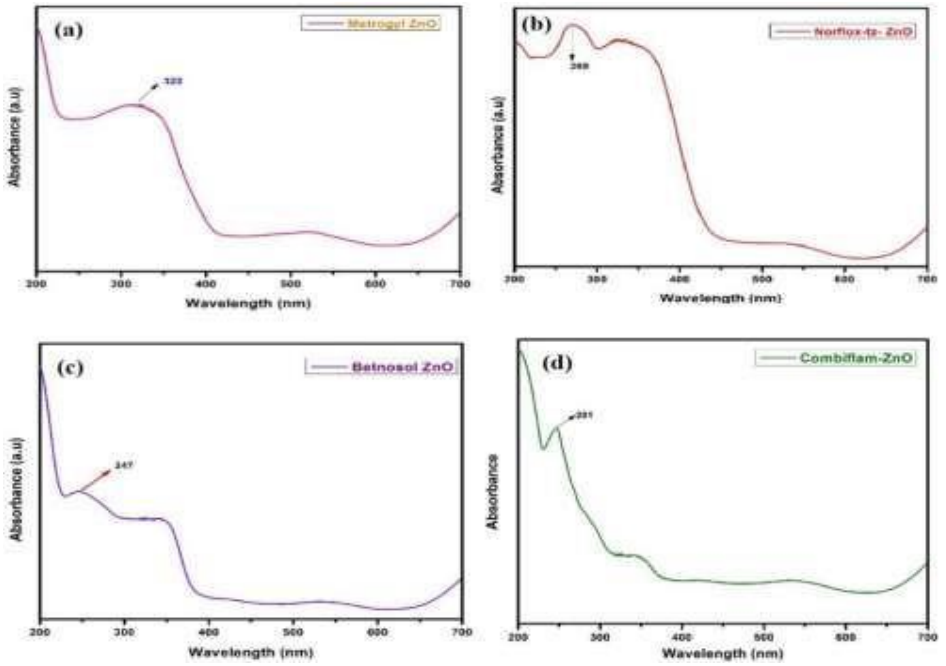


Fig. 2 Absorbance of Zinc oxide nanoparticles derived from various expired medicines.

ZnO NPs synthesized from expired pharmaceuticals Metrogyl, Norflox-TZ, Betnesol, and Combiflam have determined band gap values of 1.5 eV, 1.47 eV, 1.5 eV, and 1.48 eV, respectively. These values are lower than those reported by Klinton Davis et al. for sol-gel-synthesised ZnO NPs [19]. The use of a green production process and the use of expired medications such as Metrogyl, Norflox-tz, Betnesol, and Combiflam are likely to have contributed to the observed decrease in the band gap of the resultant ZnO NPs. The novelty of this present research is that such semiconductor nature of energy band has been found using waste expire medicine as reducing agent. The range of band gap obtained in the present study reflects the semiconducting behaviour of ZnO nanoparticles. Among the four samples ZnO NPs synthesized using Norflox-Tz exhibited the lowest band gap. The reason for such a decrease may be due to the decrease in crystallite size in accordance with the Brus effective mass model [23-26]. The relationship of band gap with the particle size may be given as follows:

$$E_g = E_g^{bulk} + \frac{\hbar^2\pi^2}{2er^2}\left(\frac{1}{m_e} + \frac{1}{m_h}\right) - \frac{18e^2}{4\pi\epsilon_0\epsilon_r}, (2)$$

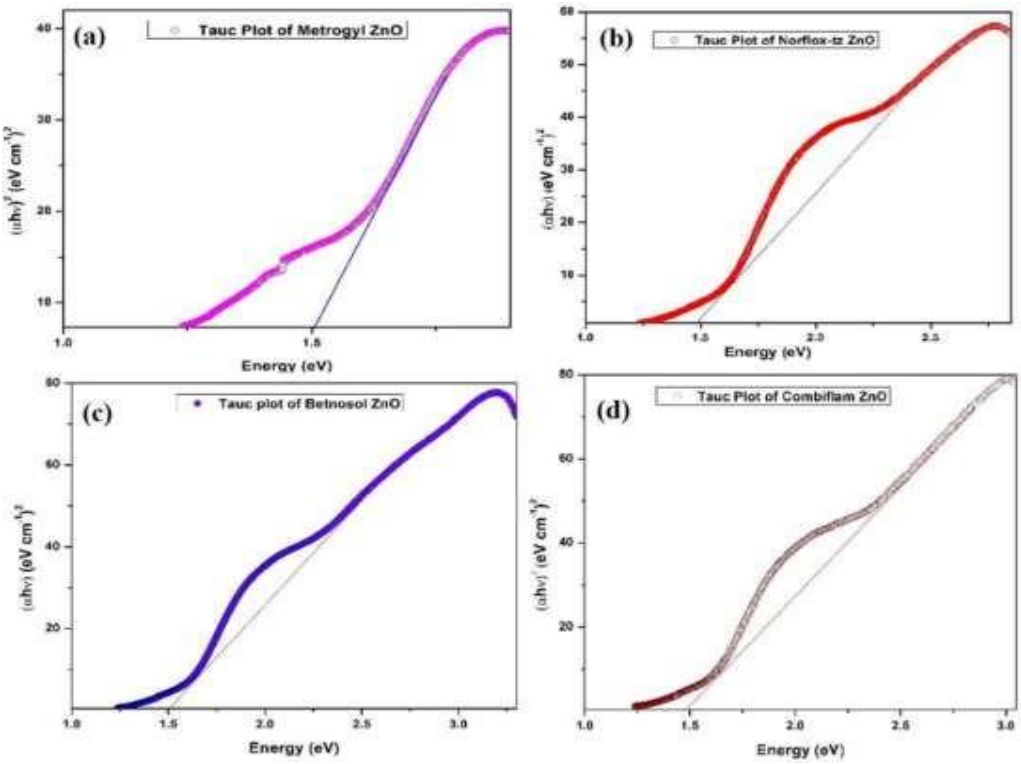


Fig. 3 Band gap of ZnO NPs synthesized by expired medicine (a) Metrogyl (b) Norflox-TZ (c) Betnosol (d) Combiflam

3.2 X-ray diffraction (XRD) analysis

The phase formation of ZnO NPs was confirmed through data analysis of X-ray diffraction (XRD). The X-ray diffraction patterns of ZnO NPs mediated by expired medicines exhibited strong peaks at room temperature. In Figure 4, the indexed XRD profile of ZnO NPs displays several distinct Bragg reflections with 2 theta (2θ) values of 31.80°, 34.20°, 36.03°, 47.29°, 56.36°, 62.63°, and 67.70°, corresponding to lattice planes (100), (002), (101), (102), (110), (103), etc. in expired medicines Metrogyl, Norflox-tz, Betnesol, and Combiflam. These XRD peaks were associated with the diffraction planes of a hexagonal crystal structure belonging to P 63 m c space group. Figure 4 (b) reveals that ZnO NPs produced via Norflox-Tz mediation exhibit a higher degree of crystallinity. The presence of broad peaks indicates the formation of very small particles with a crystalline behaviour. Besides, ZnO NPs synthesized by Norflox, the same synthesized using Metrogyl also shows a moderate degree of crystallinity. The diffraction parameters have matched with the COD ID 2300116 (Crystallography Open Database).

The following equations have been used to calculate the structural parameters of ZnO [24]:

$$n\lambda = 2d\sin\theta\,, (3)$$

$$\frac{1}{d^2} = \frac{4}{3}\left(\frac{h^2+hk+k^2}{a^2}\right) + \frac{l^2}{c^2}\,, (4)$$

Using the planes (100) and (002) the lattice constants a = b, and c were found to be 3.246 Å and 5.182 Å, repectively. Table 1 illustrates the d-spacing and hkl values against each 2θ values. The calculated values resemble with the ideal XRD parameters of ZnO. Hence the phase formation of ZnO can be easily defended.

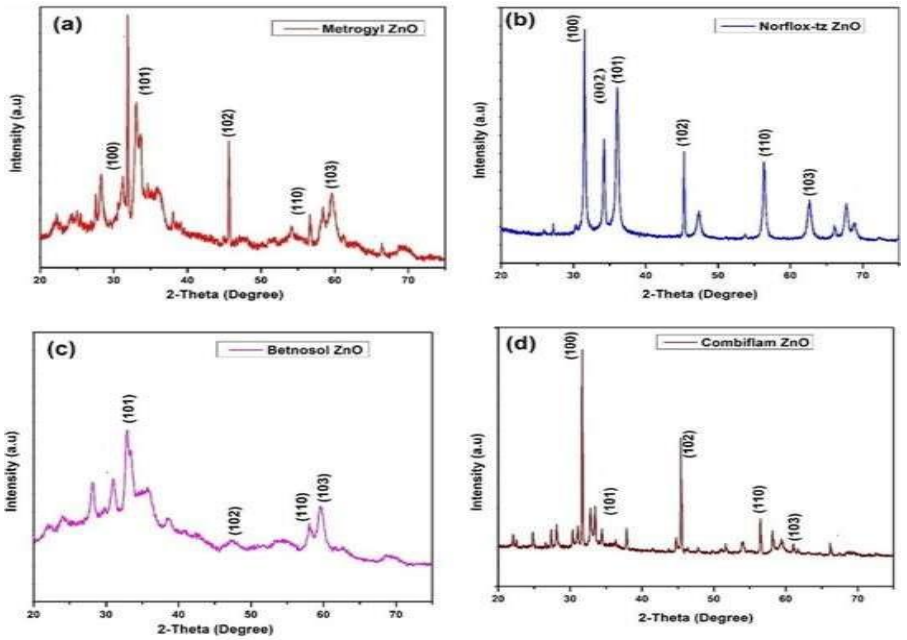


Fig. 4 XRD spectrum of ZnO NPs synthesized by expired medicine (a) Metrogyl (b) Norflox TZ (c) Betnosol (d) Combiflam

Table 1: XRD parameters of ZnO (Norflox-Tz)

| 2Theta | d-calculated | Hkl |
|---|---|---|
| 31.80 | 2.811 | 1 0 0 |
| 34.20 | 2.591 | 0 0 2 |
| 36.03 | 2.468 | 1 0 1 |
| 47.29 | 1.904 | 1 0 2 |
| 56.36 | 1.629 | 1 1 0 |
| 62.68 | 1.469 | 1 0 3 |
| 67.70 | 1.380 | 1 1 2 |

The size estimation of nanoparticles and strain values was derived from the line broadening of the (100), (002), (101), (102), (110), and (103) reflections using the Williamson-Hall plot equation [27, 28]:

$$\beta\cos\theta = K\lambda/D + 4\varepsilon\sin\theta, (5)$$

where β is the full width at half maximum, λ is the wavelength of X-rays.

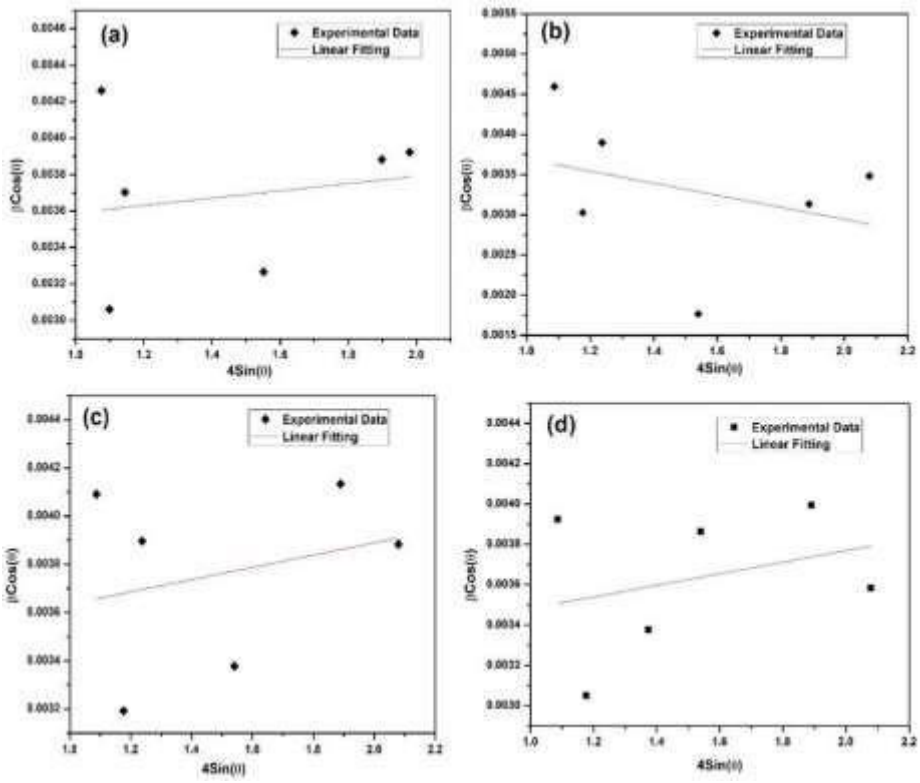


Fig 5. W-H Plot of ZnO NPs (a) Metrogyl (b) Norflox TZ (c) Betnosol (d) Combiflam

Table 2- W-H parameters of ZnO NPs

| Sr.No | ZnO NPs through expired medicine | Strain ($\times 10^{-4}$) | Crystallite Size (nm) |
|---|---|---|---|
| 01 | Metrogyl | 2.22 | 40.9 |
| 02 | Norflox-TZ | 2.19 | 39.92 |
| 03 | Betnosol | 2.55 | 41.02 |
| 04 | Combiflam | 2.87 | 43.46 |

The slope gradient, 4 ε Sin(θ), represents strain effects, while the y-intercept, (K λ) / D, indicates the crystalline size of ZnO NPs mediated through expired medicine. The crystallite size and strain value of ZnO NPs mediated through expired medicine Metrogyl, Norflox-TZ, Betnosol and Combiflam is illustrated in Table 2. Figure 5 shows the W-H plots of ZnO

nanoparticles.

3.3 Surface analysis using Scanning Electron Microscope (SEM)

In order to obtain the SEM micrograph of the sample, powder form of ZnO NPs derived through expired Metrogyl and Norflox-Tz was sprinkled on the carbon coated Cu grid by sprinkling a very small amount of the sample on the grid. Since, ZnO synthesized using Metrogyl and Norflox-Tz has the highest crystallinity, the SEM investigation of these samples have only been done in the present study.

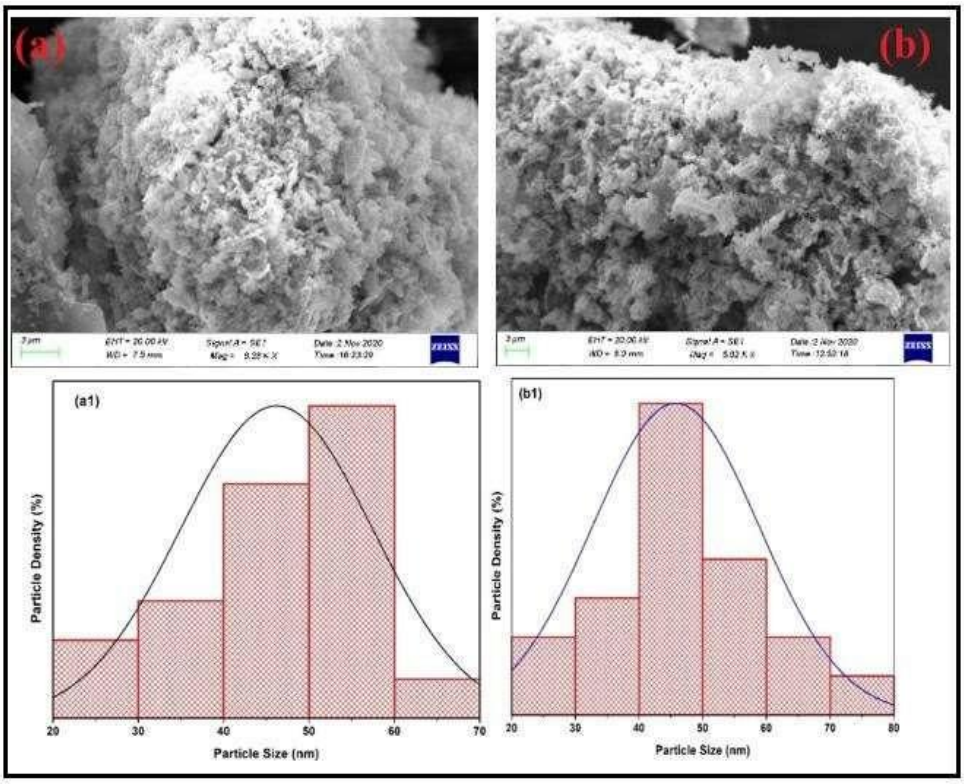


Fig 6(a-b): SEM micrograph and histogram of ZnO synthesized by expired medicine (a) Metrogyl (b) Norflox TZ

In order to make the material conductive, it is coated with gold using sputtering coating machine. And hence, SEM micrograph of the ZnO NPs mediated through Metrogyl and Norflox-Tz is obtained. Figure 6 (a) and (b) represents the morphological image of ZnO nanoparticles synthesized through Metrogyl and Norflox-Tz respectively. From the figure it can be inferred that the sample shows flower-like structure [27]. Agglomeration in the NPs is seen and also the distribution of nano structures is not uniform. The approximate crystallite size of ZnO NPs synthesized through Metrogyl and Norflox-Tz was found to be 46 nm and 45 nm respectively. For the estimation of particle size ImageJ software was utilized by scanning various surface area and analyzing it one by one [28]. The related histogram of the material is also shown by figure (a1) and (b1). Interparticle interaction is almost same in both the cases.

3.3 FTIR Analysis

The FTIR spectra, which involve a spectral range of 500-4000 $cm^{-1}$, provide the functional groups involved in the synthesized ZnO NPs. The Zn-O wavenumbers found in the ZnO NPs are consistent with previous research [29-30] and are shown in Figure 7.

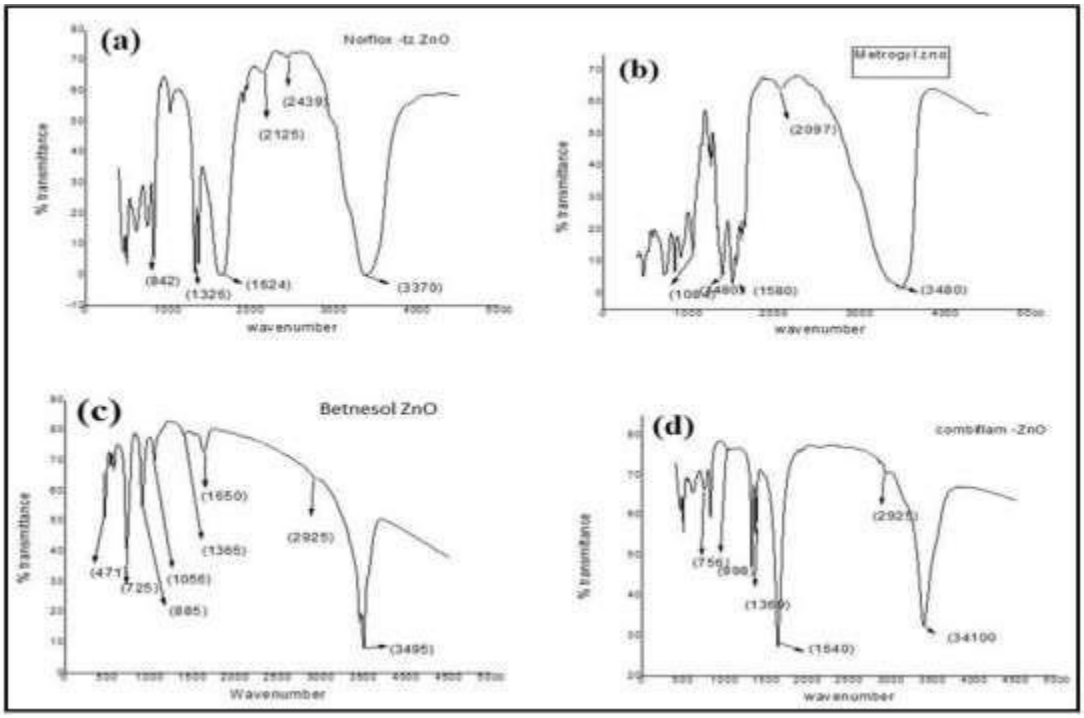


Fig 7. FTIR spectrum of ZnO NPs (a) Norflox TZ (b) Metrogyl (c) Betnosol (d) Combiflam

The wavenumbers between 471 and 885 $cm^{-1}$ indicate ZnO stretching vibrations. The significant peak seen between 3370 $cm^{-1}$ and 3495 $cm^{-1}$ corresponds to the O-H band and the C=O stretch, indicating the presence of aliphatic carboxylic acid molecules. The existence of an aromatic ring is shown by the wavenumbers between 1554 $cm^{-1}$ and 1558 $cm^{-1}$. A band between 1028 $cm^{-1}$ and 1033 $cm^{-1}$, represent C-O stretching vibrations. The doublet absorption between 2927 $cm^{-1}$ and 2931 $cm^{-1}$ corresponds to aromatic aldehyde C-H stretching vibrations. The metal oxide vibrations present in the FTIR spectra indicate the phase formation of ZnO nanoparticles and it is in accordance with the XRD results. Table 3 displays various FTIR vibrations in ZnO nanoparticles. The existence of terpenoid group chemicals in the extract of expired pharmaceuticals is suggested by the observed bands. The FTIR measurement shows that alcohols, ketones, aldehydes, and carboxylic acids are encapsulated within the synthesized nanoparticles.

Table 4: FTIR vibrations of ZnO.

| Wavenumbers | Vibration mode |
|---|---|
| 471-886 | ZnO stretching |
| 1028-1033 | C-O stretching |
| 1554-1558 | C=C stretching and C=O stretching (aromatic) |
| 2927-2931 | C-H stretching |
| 3370-3495 | O-H and C=O stretching |

### 3.4 Antimicrobial activity

Antimicrobial activity was performed by agar well diffusion method, with slight modifications. Freshly prepared molten Muller Hinton Agar (MHA) media was used for bacterial culture and Potato Dextrose Agar (PDA) media was used for fungal culture. Both the media were poured to uniform depth of 5 mm and allowed to cool at room temperature [33-35]. After solidification, wells were made in MHA media by 6 mm sterilized cork borer. 1-2 drops of media were poured in the bottom with the help of sterile micropipette. 1-2 $\times 10^7$ cfu/mL of test microorganisms were spread on the surface of MHA media using a glass spreader. 30 µL of ZnO-NPs concentrations were filled in three wells. DMSO was also used as negative control. The plates were then incubated for 24 h at 37 °C for bacterial culture and 48 h at 25 °C for fungal culture.

#### 3.4.1 Antibacterial activity

The experiment was carried out using the agar disc diffusion technique. [36] ZnO NPs were tested for antibacterial activity against common infectious bacteria, including Pseudomonas aeruginosa (P. aeruginosa), Staphylococcus aureus (S. aureus), Escherichia coli (E. coli), and Bacillus cereus (B. cereus). Figure 8 shows the antibacterial activity of the synthesized ZnO NPs.

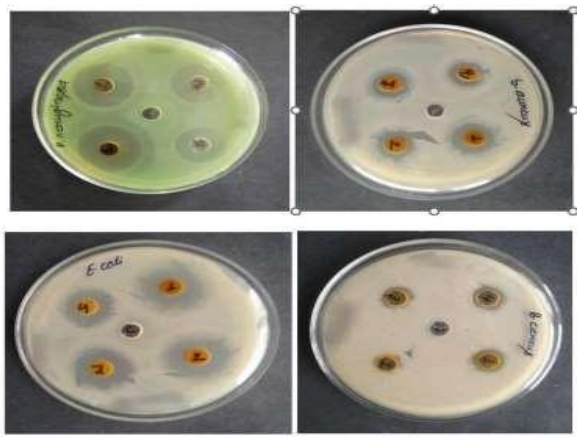

Fig 8. Antibacterial activity of ZnO nanoparticles (a) P. aeruginosa (b) S. aureus (c) E. coli

(d) B. cereus

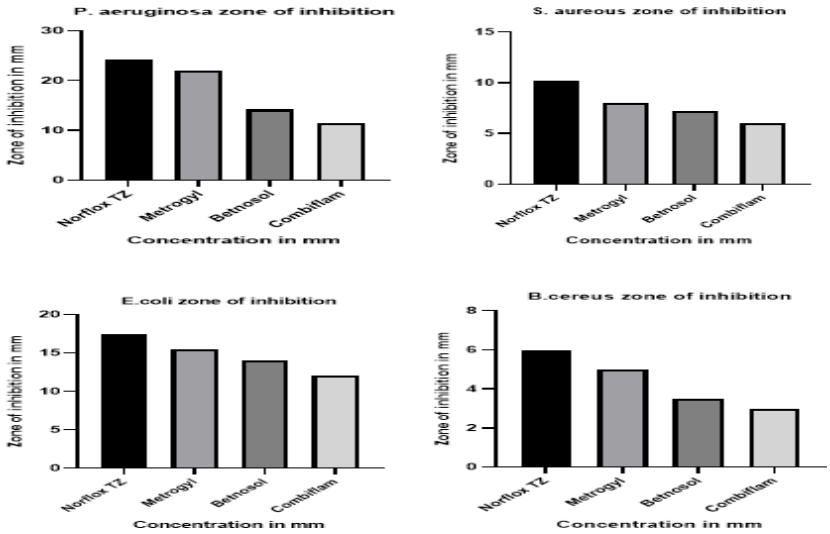


Fig 9. Graphical representation of disc method of zone inhibition of ZnO nanoparticles

The findings clearly reveal that the nanoparticles had an antibacterial effect that varied with dosage (Tables 5 and 6). All four ZnO NPs synthesized from expired medications were effective against P. aeruginosa, S. aureus, E. coli, and B. cereus. Notably, ZnO NPs synthesized using Norflox TZ and Metrogyl were more effective compared to those synthesized using Combiflam and Betnosol. The gram-negative bacterium P. aeruginosa exhibited the largest zone of inhibition, while the gram-positive bacterium B. cereus showed the smallest zone of inhibition. Previous research has indicated various modes of nanoparticle activity against gram-positive and gram-negative bacteria, which have been linked to differences in structural composition. A graphical representation of the zone of inhibition is shown in Figure 8, and Figure 9 presents the graphical inhibition zone for the bacteria analyzed in this study. The zinc oxide nanoparticles demonstrated the capability to inhibit microbial growth, as evidenced by their in-vitro antimicrobial activities [30-31].

Table 5. Antibacterial activity of synthesized ZnO nanoparticles against pathogenic bacteria.

| S. No. | Name of Bacteria | Zone of inhibition in mm | | |
|---|---|---|---|---|
| | | Norflox TZ ZnO NPs (30mg/ml) | Metrogyl ZnO NPs (30mg/ml) | Control |
| 1. | P. aeruginosa | 24.2 ± 1.16 | 22.0±0.88 | --- |
| 2. | S. aureus | 10.2 ± 0.88 | 8.1±0.58 | --- |
| 3. | E. coli | 17.4 ± 1.16 | 15.5±1.00 | --- |
| 4. | B. cereus | 6.0 ± 0.58 | 5.0±0.58 | --- |

Table 6. Antibacterial activity of synthesized ZnO nanoparticles against pathogenic bacteria

| S. No. | Name of Bacteria | Zone of inhibition in mm | | |
|---|---|---|---|---|
| | | Betnosol ZnO NPs (30mg/ml) | Combiflam ZnO NPs (30mg/ml) | Control |
| 1. | P. aeruginosa | 14.2± 1.10 | 11.5 ± 0.91 | --- |
| 2. | S. aureus | 7.22 ± 0.88 | 6.0 ± 1.16 | --- |
| 3. | E. coli | 14.0 ± 1.00 | 12.1± 0.88 | --- |
| 4. | B.cereus | 3.5 ± 058 | 3.0± 0.58 | --- |

### 3.4.2 Antifungal activity

The experiment was carried out using the agar disc diffusion technique. ZnO NPs were tested for antifungal activity against common infectious fungi such as Aspergillus niger (A. Niger), Candida albicans (C. albicans), Fusarium oxysporum (F. oxysporum), and Penicillium citrinum (P. citrinum). The antifungal activity of ZnO NPs was evaluated and is displayed in Figure 10, with the inhibition data provided in Tables 7 and 8. Among the four fungal strains studied for antifungal activity, A. niger showed zones of inhibition measuring 26 mm, 22 mm, 20 mm, and 0 mm; C. albicans showed 18 mm, 16 mm, 14 mm, and 12 mm; F. oxysporum showed 18 mm, 18 mm, 16 mm, and 18 mm; and P. citrinum showed 28 mm, 26 mm, 24 mm, and 18 mm for ZnO synthesized using Norflox TZ, Metrogyl, Betnosol, and Combiflam, respectively.

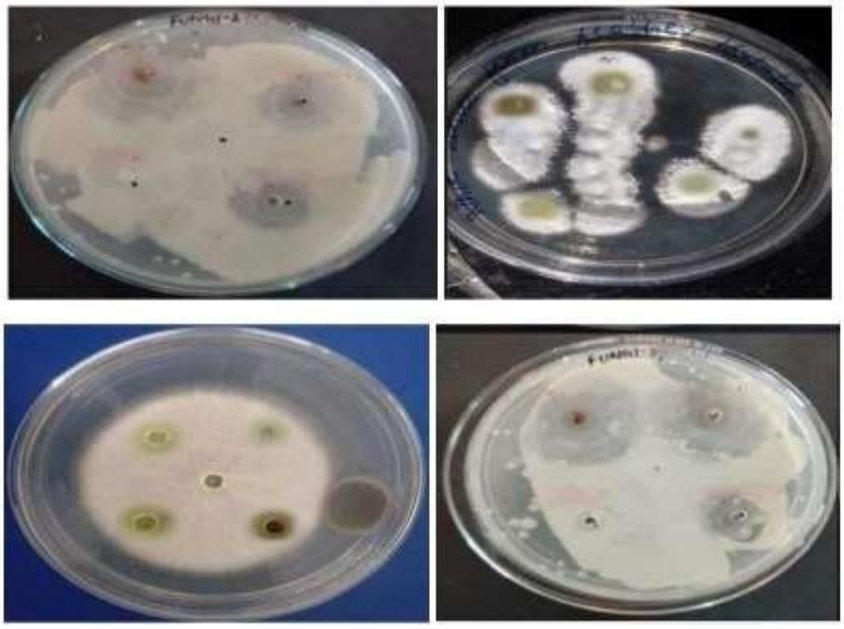

Fig 10. Antifungal activity of ZnO nanoparticles against (a) A. niger (b) C. albicans (c) F. oxysporium (d) P. citrinum.

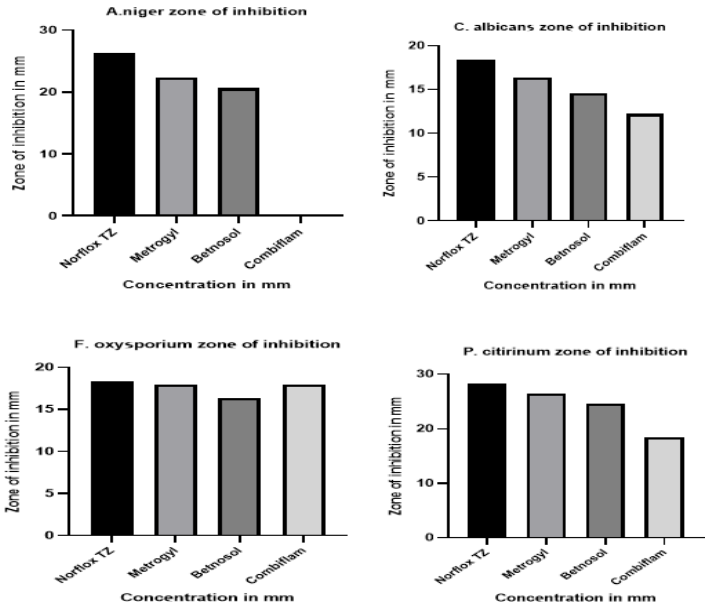


Fig 11. Graphical representation of disc method of zone inhibition of ZnO nanoparticles against various fungi.

Table 7. Antifungal activity of synthesized ZnO nanoparticles

| SI. No. | Zone of inhibition in mm | | | |
|---|---|---|---|---|
| | Name of Fungi | Norflox TZ ZnO NPs (30mg/ml) | Metrogyl ZnO NPs (30mg/ml) | Control |
| 1 | A. niger | 26.2± 1.16 | 22.4± 97 | --- |
| 2 | C. albicans | 18.4± 1.10 | 16.4± 1.12 | --- |
| 3 | F. oxysporium | 18.4± 1.14 | 18± 0.98 | --- |
| 4 | P. citirinum | 28.2± 68 | 26.4± 0.88 | --- |

Table 8. Antifungal activity of synthesized ZnO nanoparticles

| SI. No. | Zone of inhibition in mm | | | |
|---|---|---|---|---|
| | Name of Fungi | Betnosol ZnO NPs (30 mg/ml) | Combiflam ZnO NPs (30 mg/ml) | Control |
| 1 | A. niger | 20.6± 0.62 | --- | --- |
| 2 | C. albicans | 14.6± 1.12 | 12.2± 1.10 | --- |
| 3 | F. oxysporium | 16 ± 1.08 | 18.4± 0.88 | --- |
| 4 | P. citirinum | 24.6± 0.98 | 18.4± 0.92 | --- |

The reasons behind antimicrobial growth inhibition can be attributed to the membrane lysis occurring as a result of interaction between the ZnO NPs and negative charges on the cell membranes of the organism (bacteria and fungi), enhanced membrane permeability, internalization of NPs due to loss of proton motive force and uptake of toxic dissolved zinc

ions as evident from literature reports.[37, 38]

## 4. Conclusions:

In this study, a simple and environmentally friendly method for producing Zinc oxide (ZnO) nanoparticles (ZnO NPs) using extracts from expired pharmaceuticals (Norflox-TZ, Metrogyl, Betnosol, and Combiflam) as novel agents for reduction and stabilization was introduced. This approach has the potential to be a cost-effective and efficient solution for addressing environmental waste issues. X-ray diffraction (XRD) examination indicates the successful formation of ZnO nanoparticles with hexagonal crystal system (ZnO NPs), where the average crystallite size has been found ranging from 40 to 44 nm. The highest crystallinity and the lowest crystallite size was recorded for ZnO NPs synthesized using Norflox-Tz. UV-visible spectra revealed absorption peaks in the UV area and reduced band gaps for ZnO NPs ranging from 1.47 to 1.5 eV, which may reveal the semiconducting behaviour of nanoparticles. The FTIR spectroscopy studies revealed the molecular oxide bonds ranging from 471 to 885 $cm^{-1}$. The research findings also highlighted the antimicrobial efficacy of ZnO nanoparticles (NPs) synthesized from various expired medications. The antibacterial activity showed that P. aeruginosa had the highest inhibition zone (24.2 ± 1.16 mm) when treated with ZnO NPs synthesized from Norflox TZ, while B. cereus displayed the smallest inhibition zone (6.0 ± 0.58 mm). For antifungal activity, P. citrinum exhibited the largest inhibition zone (28.2 ± 0.68 mm) with Norflox TZ-derived ZnO NPs, whereas C. albicans showed lower inhibition zones, with values as low as 12.2 ± 1.10 mm for Combiflam-synthesized ZnO NPs. These findings indicate that ZnO NPs synthesized using Norflox TZ and Metrogyl were more effective against a range of microorganisms compared to those from Betnosol and Combiflam. The study supports the potential of ZnO NPs as strong antimicrobial agents with semiconductor properties emphasizing the importance of further research to optimize synthesis for enhanced activity and its possible applications.

Acknowledgements: The authors are grateful to Aryabhatta Knowledge University, Patna and Dept. of Education, Govt. of Bihar for having such an amenity related to nanostructured material synthesis and characterization. SM is grateful to DST SERB-SURE grant (SUR/2022/004419) for research in nanomaterials field.

Conflict of Interest

The authors do not have any conflict of interest.

## References

[1] K. Kavitha, S. Baker, D. Rakshith, H.U. Kavitha, R.H.C. Yashwantha, B.P. Harini, S. Satish, Plants as green source towards synthesis of nanoparticles, Int. Res. J. Biol. Sci. 2 (6) (2013) 66–76.

[2] K. Krause, Pharmaceutical potentials: praying over medicines in Pentecostal healing, Ghana Stud. 15-16 (2014) 223–250.
[3] M. Singhal, V. Chhabra, P. Kang, D.O. Shah, Synthesis of ZnO nanoparticles for varistor application using Zn-substituted aerosol OT microemulsion, Mater. Res. Bull. 32 (2) (1997) 239–247.
[4] K. Schilling, B. Bradford, D. Castelli, E. Dufour, J.F. Nash, W. Pape, S. Schulte, I. Tooley, J. van den Bosch, F. Schellauf, Human safety review of nano titanium dioxide and zinc oxide, Photochem. Photobiol. Sci. 9 (4) (2010) 495–509.
[5] G.E.J. Poinern, S.K. Tripathy, S. Sharma, D. Fawcett, M. Shah, Green synthesis of metallic nanoparticles via biological entities, Materials 8 (2015) 7278–7308.
[6] M. Anandan, G. Poorani, P. Boomi, K. Varunkumar, K. Anand, Chuturgoon A. Anil, M. Saravanan, Prabu H. Gurumallesh, Green synthesis of anisotropic silver nanoparticles from the aqueous leaf extract of Dodonaea viscosa with their antibacterial and anticancer activities, Process Biochem. 80 (2019) 80–88.
[7] Mani Divyaa, Baskaralingam Vaseeharana, Muthukumar Abinayaa, Sekar Vijayakumara, Marimuthu Govinda, Biopolymer gelatin-coated zinc oxide nanoparticles showed high antibacterial, antibiofilm and anti-angiogenic activity, J. Photochem. Photobiol. B 178 (2018) 211–218.
[8] Hamed Barabadi, Muhammad Ovais, Zabta Khan Shinwari, Muthupandian Saravanan, Anti-cancer green bionanomaterials: present status and future prospects, Green Chem. Lett. Rev. 10 (4) (2017) 285–314.
[9] Karuppannan Periyasamy, Saravanan Kaliyaperumal, Eco-friendly synthesis of silver nanoparticles using Ventilago maderaspatana (GAERTN), their morphological characterization, Int. J. ChemTech Res. 10 (9) (2017) 01–06.
[10] Hamed Barabadi, Ahad Alizadeh, Muhammad Ovais, Amirhossein Ahmadi, Zabta Khan Shinwari, Muthupandian Saravanan, Efficacy of green nanoparticles against cancerous and normal cell lines: a systematic review and meta-analysis, IET Nanobiotechnology 12 (4) (2017) 377–391.
[11] P.C. Nagajyothi, T.N. Minh, T.V.M. Sreekanth, Jae-il Lee, Dong Joo Lee, K.D. Lee, Green route biosynthesis: characterization and catalytic activity of ZnO nanoparticles, Mater. Lett. 108 (2013) 160–163.
[12] K. Durgadevi, R. Gowri, S.T. Mini, V. Ramamurthy, A study of biosynthesis and characterization of silver nanoparticles from Cassia auriculata, Int. J. Res. Anal. Rev. 5 (4) (2018) 442–447.
[13] Singh Sonu Kumar, Rakesh Kumar Singh, P. K. Verma, Md Irfanul Haque Siddiqui, Masood Ashraf Ali, Aniket Manash, Tuning of structural, elastic, luminescence, magnetic, and multiferroic properties of rare earth Ce3+ substituted strontium hexaferrite Ceramic magnetic nanomaterials for its industrial applications, Applied Physics A: Materials Science & Processing. (2021) 127:754.
[14] H.H. Park, Y.J. Choi, Direct patterning of SnO2 composite films prepared with various contents of Pt nanoparticles by photochemical metal-organic deposition, Thin Solid Films 519 (2011) 6214–6222.
[15] P. Ramesh, K. Saravanan, P. Manogar, J. Johnson, E. Vinoth, M. Mayakannan, Green synthesis and characterization of biocompatible zinc oxide nanoparticles and evaluation of its antibacterial potential, Elsevier: Sensing and Bio-Sensing Research 31 (2021) 100399.
[16] Gikonyo D, Gikonyo A, Luvayo D, Ponoth P. Drug expiry debate: the myth and the reality. Afr Health Sci. 2019 Sep;19 (3):2737-2739
[17] Naveen Kumar, Shashi Bhushan, Niraj Kumari, Anal K. Jha, Green synthesis of silver nanoparticles using Expired medicines and assessment of its antibacterial activity: A
Novel Approach, AIP Conference Proceedings (2020) 2220, 020067.
[18] J. Santhoshkumar, Kumar S. Venkat, S. Rajeshkumar, Synthesis of zinc oxide nanoparticles using plant leaf extract against urinary tract infection pathogen, Resour. Effic. Technol. 3 (2017) 459–465.
[19] Klinton Davis, Ryan Yarbrough, Michael Froeschle, Jamel White, Hemali Rathnayake, Band Gap Engineered Zinc Oxide Nanostructures: Via a Sol-Gel Synthesis of Solvent Driven Shape-Controlled Crystal Growth. RSC Adv. 2019, 9 (26), 14638–14648.
[20] Z.M. Khoshhesab, M. Sarfaraz, M.A. Asadabad, Preparation of ZnO nanostructures by chemical precipitation method, Synth. React. Inorg. Met. 41 (7) (2011) 814–819.
[21] S. Talam, S.R. Karumuri, N. Gunnam, Synthesis, characterization, and spectroscopic properties of ZnO nanoparticles, ISRN Nanotechnol. (2012) 372505.
[22] J. Zhou, F. Zhao, Y. Wang, Y. Zhang, L. Yang, Size controlled synthesis of ZnO nanoparticles and their

photoluminescence properties, J. Lumin. 122–123 (1–2) (2007) 195–197.
[23] Kumar, V., Singh, R.K., Sarkar, K., Kumari, R., Shah, J., Kotnala, R.K.: A Novel Ag-MgFe2O4 nanocomposite based Hydroelectric Cell: Green energy source illuminating the future. Journal of Alloys and Compounds. 175032 (2024).
[24] Sarkar, K., Harsh, H., Rahman, Z., Kumar, V.: Enhancing the structural, optical, magnetic and ferroelectric properties of perovskite BiFeO3 through metal substitution. Chemical Physics Impact. 8, 100478 (2024).
[25] Sarkar, K., Kumar, V.: Luminescence and dielectric investigations of crystalline niobate nanoceramics prepared through aqueous chemical process. Physica Scripta. 99, 105992 (2024).
[26] Kumar, V., Singh, R.K., Manash, A., Das, S.B., Shah, J., Kotnala, R.K.: Structural, optical and electrical behaviour of sodium-substituted magnesium nanoferrite for hydroelectric cell applications. Applied Nanoscience. 13, 4573–4591 (2022).
[27] Das S.B, Singh R.K, Kumar V, Kumar N, Singh P, Naik N.K, Structural, magnetic, optical and ferroelectric properties of Y3+ substituted cobalt ferrite nanomaterials prepared by a cost-effective sol-gel route. Mater Sci Semicond Process. 145, 106632 (2022)
[28] Shankar, U., Singh, R.K., Das, S.B. et al. Studies on the Structural Properties and Band Gap Engineering of Ag+-Modified MgFe2O4 Nanomaterials Prepared by Low-Cost Sol–Gel Method for Multifunctional Application. J Supercond Nov Magn 35, 1937–1960 (2022).
[29] Singh, R.P.; Shukla, V.K.; Yadav, R.S.; Sharma, P.K.; Singh, P.K.; Pandey, A.C. Biological approach of zinc oxide nanoparticles formation and its characterization Adv. Mater. Lett. 2011, 2, 313–317.
[30] Rao, C.N.R. Chemical Applications of Infrared Spectroscopy; Academic Press: New York and London, 1963; pp. 25–40.
[31] Ayala-Núñez NV, Lara HH, Turrent LDCI, Padilla CR. Silver nanoparticles toxicity and bactericidal efect against methicillin resistant Staphylococcus aureus: nanoscale does matter. Nanobiotechnol. 2009; 5:2–9.
[32] Prakash P, Gnanaprakasam P, Emmanuel R, Arokiyaraj S, Saravanan M. Green synthesis of silver nanoparticles from leaf extract of Mimusops elengi, Linn. for enhanced antibacterial activity against multi drug resist ant clinical isolates. Colloids Surf B Biointerfaces. 2013; 108:255–9.
[33] Biswas A, Vanlalveni C, Adhikari PP, Lalfakzuala R, Rokhum L. Biosynthesis, characterisation and antibacterial activity of Mikania micrantha leaf extract-mediated AgNPs. Micro Nano Lett 2019; 14:799 – 803. https://doi.org/10.1049/mnl.2018.5661.
[34] Biswas A, Vanlalveni C, Adhikari PP, Lalfakzuala R, Rokhum L. Green biosynthesis, characterisation and antimicrobial activities of silver nanoparticles using fruit extract of Solanum viarum. IET Nanobiotechnology 2018; 12:933 – 938. https://doi.org/10.1049/iet- nbt.2018.0050.
[35] Biswas A, Chawngthu L, Vanlalveni C, Hnamte R, Lalfakzuala R, Rokhum L. Biosynthesis of silver nanoparticles using selaginella bryopteris plant extracts and studies of their antimicrobial and photocatalytic activities. J Bionanoscience 2018; 12:227–32.
[36] Balouiri, M, Sadiki, M, Ibnsouda, S K. Methods for in vitro evaluating antimicrobial activity: A review. J Pharm Anal 2016; 6:71–79. https:// doi. org/ 10. 1016/j. jpha. 2015. 11. 005.
[37] Sirelkhatim, A, Mahmud, S, Seeni, A, Kaus, N H M, Ann, L C, Bakhori, S K M, Hasan, H, Mohamad, D. Review on Zinc Oxide Nanoparticles: Antibacterial Activity and Toxicity Mechanism. Nanomicro Lett. 2015;7(3):219-242. doi: 10.1007/s40820-015-0040-x.
[38] Sun, Q, Jianmei, L, Le, T. Zinc Oxide Nanoparticle as a Novel Class of Antifungal Agents: Current Advances and Future Perspectives. J. Agric. Food Chem. 2018; 66(43):11209–11220. https://doi.org/10.1021/acs.jafc.8b03210